Multi-critical point in a diluted bilayer Heisenberg quantum antiferromagnet

Anders W. Sandvik
Department of Physics, Åbo Akademi University, Porthansgatan 3, FIN-20500 Turku, Finland
(Dated: February 1, 2008)

The $S = 1/2$ Heisenberg bilayer antiferromagnet with randomly removed inter-layer dimers is studied using quantum Monte Carlo simulations. A zero-temperature multi-critical point (p^*, g^*) at the classical percolation density $p = p^*$ and inter-layer coupling $g^* \approx 0.16$ is demonstrated. The quantum critical exponents of the percolating cluster are determined using finite-size scaling. It is argued that the associated finite-temperature quantum critical regime extends to zero inter-layer coupling and could be relevant for antiferromagnetic cuprates doped with non-magnetic impurities.

PACS numbers: 75.10.Jm, 75.10.Nr, 75.40.Mg, 75.40.Cx

Randomly diluted quantum spin systems combine aspects of the percolation problem [1] with the physics of thermal and quantum fluctuations. In systems that can be tuned through a $T = 0$ phase transition as a function of some parameter one can hence study divergent quantum fluctuations coexisting with classical fluctuations due to percolation. A multi-critical point, where the two types of fluctuations diverge simultaneously, is realized in the transverse Ising model with dimensionality $D > 1$ [2, 3]. In models with $O(N)$ symmetry and $N > 2$ such a point was believed not to exist, because quantum fluctuations were argued to always destroy the long-range order on the percolating cluster [3]. Several studies of diluted 2D Heisenberg antiferromagnets were consistent with this scenario [4, 5, 6]. However, recent quantum Monte Carlo simulations have shown that long-range order in the 2D Heisenberg model persists until the percolation point [7, 8, 9] and that the percolating cluster is ordered as well [8, 9]. This implies that the phase transition is a classical percolation transition. It also suggests that a multi-critical point, at which the percolating cluster is quantum critical, could be reached by including other interactions. In this Letter it will be shown that the $O(3)$ multi-critical point can be realized in the Heisenberg bilayer with dimer dilution, i.e., where adjacent spins on opposite layers are removed together. This system is illustrated in Fig. 1, and a schematic $T = 0$ phase diagram is shown in Fig. 2. In analogy with quantum critical points in clean 2D Heisenberg antiferromagnets [10, 11], one can expect a finite-T universal quantum critical scaling regime to extend to couplings well beyond the $T = 0$ critical coupling g^*, possibly all the way to decoupled layers ($g = 0$). This quantum criticality could then be realized in layered antiferromagnets doped with non-magnetic impurities. It may already have been observed in $La_2Cu_{1-x}(Zn,Mg)_xO_4$, for which recent neutron scattering experiments [12] show a correlation length divergence roughly consistent with the dynamic exponent $z \approx 1.3$ extracted here.

The clean $S = 1/2$ bilayer Heisenberg model has been extensively studied in the past [13, 14]. It undergoes a quantum phase transition between an antiferromagnetic and a quantum disordered state as a function of the ratio $g = J_2/J_1$ of the inter- and intra-plane couplings. The critical coupling $g_c \approx 2.52$ and the exponents are consistent with the expected [10] classical 3D Heisenberg universality class. If the system is diluted by randomly removing single spins, the quantum phase transition is destroyed because moments are induced around the "holes" in the gapped phase. These localized moments order antiferromagnetically for all g [15]. In order to circumvent this "order from disorder" phenomenon, inter-plane dimer dilution will be considered here. A dimer is not associated with moment formation and hence there is a spin gap for large g at any dilution fraction p. When $g = 0$ the system corresponds to two independent site-diluted Heisenberg layers. In that case, it was recently shown that the sublattice magnetization on large clusters at the percolation density scales to a non-zero value in the limit

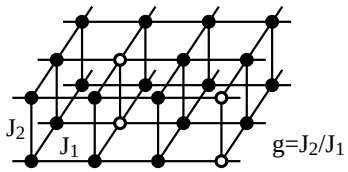

FIG. 1: The bilayer with intra- and inter-plane couplings $J_1\mathbf{S}_i \cdot \mathbf{S}_j$ and $J_2\mathbf{S}_i \cdot \mathbf{S}_k$. Solid circles represent magnetic sites ($S = 1/2$). Two removed dimers are indicated by open circles.

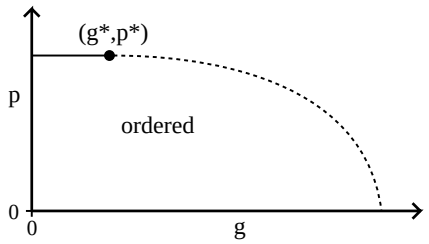

FIG. 2: Schematic $T = 0$ phase diagram for the Heisenberg bilayer with coupling g and a fraction p of the inter-plane dimers removed. Percolation and quantum phase transitions are indicated by the solid horizontal line and dashed curve, respectively. The circle indicates the multi-critical point.

of infinite cluster size [8, 9], implying a classical percolation transition. In the bilayer the long-range order on the percolating cluster can then be expected to survive up to a critical inter-layer coupling $g^* > 0$, leading to the phase diagram shown in Fig. 2.

In order to extract the multi-critical coupling g^*, quantum Monte Carlo simulations similar to those discussed in Ref. 9 were carried out at the percolation point ($p^* \approx 0.4072538$ [16]). Two types of boundary conditions were used. In periodic $L \times L$ systems, dimers were removed with probability p^* and the largest cluster of connected dimers was studied. These clusters have a varying number N_1 of dimers, with $\langle N_1 \rangle \sim AL^d$, where the fractal dimension $d = 91/48$ [1] and $A \approx 0.67$. Clusters were also constructed at fixed size N without boundary imposed shape restrictions [9]. In this case the corresponding length-scale is $R = N^{1/d}$. The two types of clusters will be referred to as $L \times L$ and fixed-N, respectively. A length $R = 0.81 \cdot L$ will sometimes be used for the $L \times L$ clusters, so that for a given R the average size $\langle N_1 \rangle \approx R^{1/d}$ is the same as the size of the fixed-N clusters. The calculations were carried out using the stochastic series expansion method [17]. Temperatures sufficiently low to obtain ground state properties were used for $L \times L$ clusters with L up to 64 and fixed-N clusters with N up to 1024. The results were averaged over a large number of dilution realizations; from $> 10^3$ for the largest sizes to $> 10^5$ for smaller sizes.

For a cluster with N_1 dimers ($N_2 = 2N_1$ spins), single-plane ($a = 1$) and full-system ($a = 2$) staggered structure factors and susceptibilities are defined as

$$S_a(\pi,\pi) = \frac{1}{N_a} \sum_{i,j=1}^{N_a} P_{ij} \langle S_i^z S_j^z \rangle, \quad (1)$$

$$\chi_a(\pi,\pi) = \frac{1}{N_a} \sum_{i,j=1}^{N_a} P_{ij} \int_0^\beta d\tau \langle S_i^z(\tau) S_j^z(0) \rangle, \quad (2)$$

where $P_{ij} = 1$ for sites i, j on the same sublattice and -1 for sites on different sublattices. Squared sublattice magnetizations are defined as [18] $\langle m_a^2 \rangle = \langle 3S_a(\pi,\pi)/N_a \rangle$, where $\langle\rangle$ indicates averaging over dilution realizations. The two definitions $\langle m_1^2 \rangle$ and $\langle m_2^2 \rangle$ should extrapolate to the same infinite-size value but the finite-size corrections can be different. In clean systems, it is known that the leading size correction is $\sim N^{-1/2}$ [19] and this was found to be the case also for the diluted single layer [9]. In Fig. 3, $\langle m_1^2 \rangle$ on $L \times L$ clusters is graphed versus $L^{-d/2} \sim \langle N_1 \rangle^{-1/2}$ for several values of the coupling, along with the previous $g = 0$ results. Quadratic fits are also shown. Interestingly, the sub-leading corrections become smaller, i.e., the behavior becomes more linear, as g is increased from 0. For $g = 0.1$ the data for $L = 20 - 64$ can be fitted to a purely linear form, which extrapolates to a non-zero value. In the inset of Fig. 3 it is shown that the definition $\langle m_2^2 \rangle$ has more curvature but

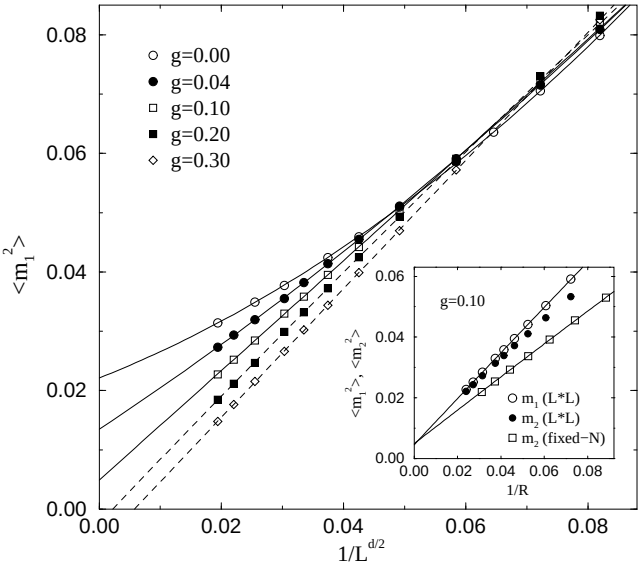

FIG. 3: Finite-size scaling of the single-plane sublattice magnetization on $L \times L$ clusters at the percolation density. In the inset, both the single-plane (m_1) and full-system (m_2) definitions of the sublattice magnetization on $L \times L$ lattices at $g = 0.10$ are shown along with m_2 for the fixed-N clusters.

approaches $\langle m_1^2 \rangle$ for the largest cluster sizes. Results for $\langle m_2^2 \rangle$ on fixed-N clusters are also shown to extrapolate to the same infinite-size value, with an over-all smaller size-correction. For $g \geq 0.2$ the extrapolations give negative values, indicating that the sublattice magnetization vanishes (the fitted forms can here not be correct for very large L, as the asymptotic behavior has to be $1/L^d$ if $\langle m_2^2 \rangle = 0$). Hence, the critical coupling $0.1 < g^* < 0.2$.

At (g^*, p^*), both $S_a(\pi,\pi)$ and $\chi_a(\pi,\pi)$ should exhibit power-law finite-size scaling. In clean systems the quantum critical scaling forms are $S \sim L^{1-\eta}$ and $\chi \sim L^{1+z-\eta}$, where $\eta \approx 0.03$ is the equal-time spin correlation function exponent and $z = 1$ is the dynamic exponent. Since the size fluctuates in the case of the $L \times L$ clusters, the statistical errors in this case are reduced in the size-normalized quantities $\langle S_a/N_a \rangle$ and $\langle \chi_a/N_a \rangle$, which therefore will be studied here. If the exponents are defined according to

$$\langle S_a(\pi,\pi)/N_a \rangle \sim R^{\gamma_S}, \quad (3)$$

$$\langle \chi_a(\pi,\pi)/N_a \rangle \sim R^{\gamma_\chi}, \quad (4)$$

the dynamic exponent can be obtained from the difference; $z = \gamma_\chi - \gamma_S$. The best over-all scaling behavior is seen in $\langle S_2/N_2 \rangle$ for the fixed-N clusters. Based on this quantity, the multi-critical point is estimated to $g^* = 0.16 \pm 0.01$, and the exponent $\gamma_S = -0.90 \pm 0.01$. A log-log plot with data for both fixed-N and $L \times L$ clusters at $g = 0.16$ is shown in Fig. 4. The $L \times L$ data have larger corrections to scaling but for the largest clusters the behavior is completely consistent with the exponent extracted from the fixed-N data. The power-law scaling in $\langle \chi_a/N_a \rangle$ sets in at larger system sizes, and

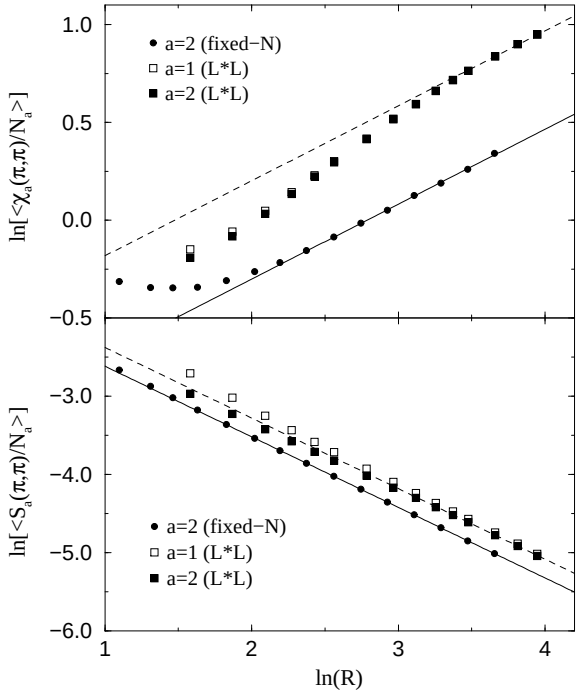

FIG. 4: Finite-size scaling of the staggered structure factors and susceptibilities. The solid lines are fits to results for the fixed-N clusters; the dashed lines have the same slopes but are shifted to match the $L \times L$ data for large R.

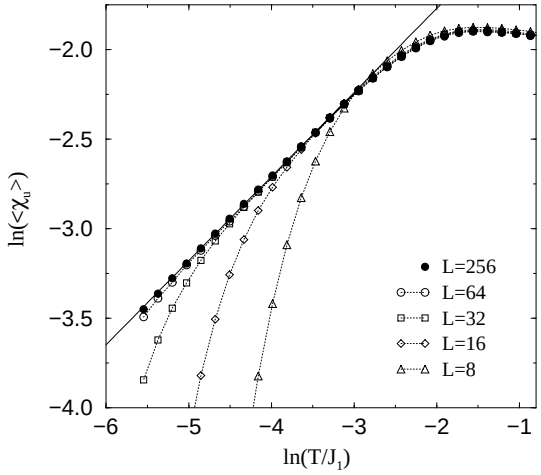

FIG. 5: Temperature dependence of the susceptibility at $g = 0.16$. Results for different system sizes are shown along with a linear fit to the $L = 256$ data. The small deviations at the lowest temperatures indicate that g^* is marginally below 0.16.

also in this case the behaviors seen for $L \times L$ and fixed-N clusters are consistent with each other. The fixed-N clusters again show a wider range of good scaling and give $\gamma_\chi = 0.38 \pm 0.03$. The dynamic exponent is hence $z = 1.28 \pm 0.02$, where correlations between γ_S and γ_χ have been taken into account in the error estimate.

According to hyper-scaling theory, the temperature dependence of the uniform magnetic susceptibility χ_u should be governed by the dynamic exponent [11, 20]:

$$\langle \chi_u \rangle = \frac{J_1}{T} \left\langle \frac{1}{N_2} \left\langle \left(\sum_{i=1}^{N_2} S_i^z \right)^2 \right\rangle \right\rangle \sim T^{D/z-1}. \quad (5)$$

Consistency with the z extracted above from $T = 0$ quantities can hence be tested in a non-trivial way. Finite-temperature calculations were carried out using sufficiently large $L \times L$ clusters to completely eliminate finite-size effects down to $T/J_1 = 1/256$. Results at $g = 0.16$ are shown on a log-log plot in Fig. 5. There is indeed a significant linear low-temperature regime, where the slope is 0.470 ± 0.005. Using $d = 91/48$ for D in Eq. (5) then gives the dynamic exponent $z = 1.29 \pm 0.01$, in full agreement with the $T = 0$ result.

Another important quantity is the spin stiffness ρ_s. It can be calculated in the simulations using the winding number fluctuations [21] in systems with periodic boundary conditions (i.e., using $L \times L$ clusters). Hyper-scaling predicts $\rho_s \sim L^{2-D-z}$ [20, 22] at a $T = 0$ critical point. At the percolation point one can expect that D should *not* be replaced by the fractal dimension d of the percolating cluster, but by its backbone dimensionality d_b, which is significantly smaller ($d_b \approx 1.643$ [23]). This is because the spin currents wrapping around the periodic clusters, in terms of which ρ_s is evaluated, only flow through the backbone. Furthermore, the above scaling form applies to systems in which the stiffness takes a finite constant value in the ordered phase. However, at p^* in the single layer (and hence for all $g < g^*$) it scales as $\langle \rho_s \rangle \sim L^{-t/\nu}$, where t is the conductivity exponent of percolation and $\nu = 4/3$ is the percolation correlation length exponent [9, 24]. The ratio $t/\nu \approx 0.983$ according to recent simulations [23]. In order to account for the "geometric" reduction, the following scaling form is tested here:

$$\langle \rho_s \rangle \sim L^{2-d_b-z-t/\nu}. \quad (6)$$

Using the value extracted for z above, the exponent $2 - d_b - z - t/\nu \approx -1.92$. Fig. 6 shows data at $g = 0.16$ along with this power-law scaling. There are clearly deviations, but it is also apparent that the numerical results are not yet in the asymptotic scaling regime. Significant corrections to the scaling law $L^{-t/\nu}$ were also seen in the single-layer case [9]. A definite test of the conjectured form (6) hence requires calculations for larger system sizes.

To summarize the results, it has been shown that a multi-critical point at the percolation threshold is realized in the dimer-diluted Heisenberg bilayer at a critical inter-plane coupling $g^* = 0.16 \pm 0.01$. The dynamic exponent z was determined using both $T = 0$ and $T > 0$ quantities, with both calculations consistent with $z = 1.28 \pm 0.02$. Vajk and Greven have recently studied the same model at $T > 0$ [25], with results in good agreement with those presented here.

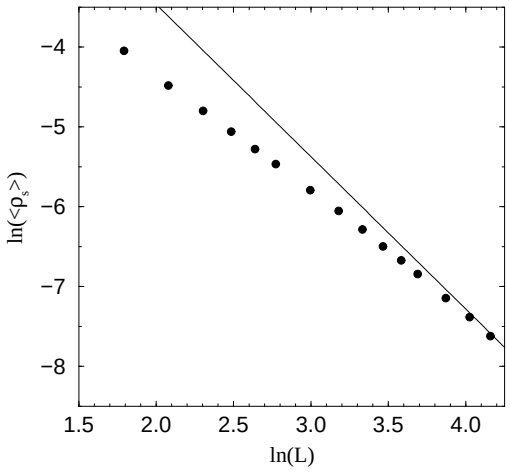

FIG. 6: Finite-size scaling of the $T = 0$ spin stiffness at $g = 0.16$. The line shows the proposed asymptotic behavior.

In analogy with finite-temperature quantum criticality in clean 2D antiferromagnets [10, 11], there should be a significant universal quantum critical regime controlled by the point (p^*, g^*). A very interesting question is then whether this universality could be observed even in a single diluted layer. The correlation length should diverge as $T^{-1/z}$ in the quantum critical regime [10, 11]. It is intriguing that this form with $z \approx 1.4$ has recently been observed at high temperatures, in simulations as well as in neutron scattering experiments on $La_2Cu_{1-p}(Zn,Mg)_pO_4$ [12]. However, since the experimental system at the percolation point corresponds to $g < g^*$ there should, in the absence of 3D effects, be a $T \to 0$ cross-over to a different dynamic exponent characterizing the line $(p = p^*, g < g^*)$. Although the percolating cluster is ordered, the exponential "renormalized classical" behavior [10, 26] cannot apply here because $\rho_s = 0$.

The $T = 0$ dynamic exponent for $(p = p^*, g < g^*)$ is governed by the properties of the percolating cluster. Since it is long-range ordered the structure factor exponent $\gamma_S = 0$ in Eq. (3). In a clean D-dimensional system with long-range order the staggered susceptibility diverges as L^{2D} [27], and if this holds also at the percolation point it would imply $\gamma_\chi = d$ in Eq. (4) and hence $z(g < g^*) = d = 91/48$. This is in contrast to the transverse Ising model, where there is activated scaling, i.e., $z = \infty$ at the percolation transition [3]. The bilayer simulations are consistent with $z(g \lesssim 0.1) = d$. Closer to g^* cross-over effects make it hard to verify this asymptotic behavior.

It should be pointed out that the bilayer coupling used here to realize a multi-critical point (p^*, g^*) is only one way to achieve this universality class. In Zn and Mg doped cuprates there may be interactions driving the system from $g = 0$ closer to such a point in an extended parameter space. The fact that the sublattice magnetization measured experimentally [12] falls significantly below the calculated curve [9] as $p \to p^*$ indicates that such couplings indeed are present.

I would like to thank I. Affleck, A. Castro Neto, M. P. A. Fisher, M. Greven, S. Sachdev, O. Sushkov, and O. Vajk for useful discussions and comments. This work was supported by the Academy of Finland (project 26175) and the Väisälä Foundation. Some calculations were done on the Condor systems at the University of Wisconsin - Madison and the NCSA in Urbana, Illinois.

[1] D. Stauffer and A. Aharony, *Introduction to Percolation Theory* (Taylor and Francis, London, 1991).
[2] A. B. Harris, J. Phys. C **7**, 3082 (1974); R. B. Stinchombe, J. Phys. C **14**, L263 (1981); R. R. dos Santos, J. Phys. C **15**, 3141 (1982).
[3] T. Senthil and S. Sachdev, Phys. Rev. Lett. **77**, 5292 (1996).
[4] C. C. Wan, A. B. Harris, and J. Adler, J. Appl. Phys. **69**, 5191 (1991); C. Yasuda and A. Oguchi, J. Phys. Soc. Jpn. **66**, 2836 (1997); J. Phys. Soc. Jpn., **68** 2773 (1999).
[5] J. Behre and S. Miyashita, J. Phys. A **25**, 4745 (1992).
[6] Y.-C. Chen and A. H. Castro Neto, Phys. Rev. B **61**, R3772 (2000).
[7] K. Kato *et al.*, Phys. Rev. Lett. **84**, 4204 (2000).
[8] A. W. Sandvik, Phys. Rev. Lett. **86**, 3209 (2001).
[9] A. W. Sandvik, Phys. Rev. B **66**, 024418 (2002).
[10] S. Chakravarty, B. I. Halperin, and D. R. Nelson, Phys. Rev. Lett. **60**, 1057 (1988); Phys. Rev. B **39**, 2344 (1989).
[11] A. V. Chubukov, S. Sachdev and J. Ye, Phys. Rev. B **49**, 11919 (1994).
[12] O. P. Vajk, P. K. Mang, M. Greven, P. M. Gehring, and J. W. Lynn, Science **295**, 1691 (2002).
[13] K. Hida, J. Phys. Soc. Jpn. **59**, 2230 (1990); A. J. Millis and H. Monien, Phys. Rev. Lett. **70**, 2810 (1993).
[14] A. W. Sandvik and D. J. Scalapino, Phys. Rev. Lett. **72** 2777 (1994); P. V. Shevchenko, A. W. Sandvik, and O. P. Sushkov, Phys. Rev. B, **61**, 3475 (2000).
[15] S. Wessel, B. Normand, M. Sigrist, and S. Haas, Phys. Rev. Lett. **86**, 1086 (2001).
[16] M. E. J. Newman and R. M. Ziff, Phys. Rev. Lett. **85**, 4104 (2000).
[17] A. W. Sandvik, Phys. Rev. B **59**, R14157 (1999).
[18] J. D. Reger and A. P. Young, Phys. Rev. B **37**, 5978 (1988).
[19] D. A. Huse, Phys. Rev. B **37** 2380 (1988).
[20] M. P. A. Fisher, P. B. Weichman, G. Grinstein, and D. S. Fisher, Phys. Rev. B **40**, 546 (1989).
[21] A. W. Sandvik, Phys. Rev. B **56**, 11678 (1997).
[22] M. Wallin, E. S. Sørensen, S. M. Girvin, and A. P. Young, Phys. Rev. B **49**, 12115 (1994).
[23] P. Grassberger, Physica A **262**, 251 (1999).
[24] A. B. Harris and T. C. Lubensky, Phys. Rev. B **35**, 6964 (1987).
[25] O. P. Vajk and M. Greven, cond-mat/0206356.
[26] A. L. Chernyshev, Y. C. Chen, A. H. Castro Neto, Phys. Rev. B **65**, 104407 (2002).
[27] P. Hasenfratz and F. Niedermayer, Z. Phys. B **92**, 91 (1993).
[28] A. B. Harris, J. Phys. C **7**, 1671 (1974).